

# Enhanced Uranium Sorption on Aluminum Oxide Pretreated with Arsenate. Part I: Batch Uptake Behavior

YUANZHI TANG\*<sup>†</sup> AND  
RICHARD J. REEDER

Department of Geosciences and Center for Environmental  
Molecular Science, State University of New York,  
Stony Brook, New York 11794-2100

Received August 25, 2008. Revised manuscript received  
March 10, 2009. Accepted April 14, 2009.

We explored mechanisms for increasing U(VI) sorption by pretreating alumina surfaces with arsenate, which has a high affinity for binding with uranyl and is an analog for phosphate. Batch experiments were conducted at pH ~4 by pretreating a  $\gamma$ -alumina surface with arsenate, followed by the addition of uranyl. Parallel experiments were conducted with different alumina loadings as well as As and U concentrations. Results show positive correlations between U(VI) uptake and  $[As]_{in}/[U]_{in}$  (ratio between the initial As solution concentration for pretreatment and the initial U solution concentration), suggesting the formation of ternary surface complexes and/or precipitates. Desorption experiments show partial irreversibility of the adsorbed U, suggesting less likelihood of remobilization. The pretreatment process results in enhanced U uptake and enhanced stability of the sorbed U, and provides a basis for designing other treatment processes for selective remediation applications.

## 1. Introduction

Contamination and migration of uranium in the natural environment have raised great concerns among scientists from different research areas. Uranium contamination occurs mainly at nuclear waste management facilities, uranium mining and milling sites, heavy industrial sites, and former nuclear weapons complexes. Understanding its transport behavior is important for assessing the potential risks posed by long-term storage of nuclear waste and also for determining the migration of natural radioactive materials in the geologic environment close to population centers.

Among the multiple oxidation states occurring in solid and aqueous forms in the environment, U(VI) is the stable oxidation state in oxidizing environments, existing almost exclusively as uranyl ( $UO_2^{2+}$ ) at surface conditions. It is more soluble and mobile than the other common oxidation state, U(IV) (1, 2). Sorption of uranyl to mineral surfaces is one of the most important mechanisms by which its mobility can be retarded in the surface and subsurface geological environments (3). Sorption is dependent on factors such as the nature of the mineral surface, availability of surface sites, and solution composition. The presence of other organic or inorganic ligands may strongly influence the speciation of

uranyl ions and, therefore, its uptake behavior by mineral surfaces (2).

Previous studies have shown that pretreating mineral surfaces with inorganic anions that have strong affinities for mineral surfaces (e.g., phosphate and sulfate) and/or metal ions can have pronounced effects on metal sorption. For example, presorbed phosphate has been shown to enhance uptake in several metal–mineral systems such as  $Pb^{2+}$ –goethite and  $Pb^{2+}$ –boehmite (4),  $Cd^{2+}/Cu^{2+}$ –goethite (5, 6),  $Dy^{3+}/Gd^{3+}$ –boehmite (7), and  $Pb^{2+}/Cu^{2+}/Zn^{2+}/Cd^{2+}$ –kaolinite (8–10). The enhancement in sorption is usually shown to be pH-dependent, with greatest enhancement occurring at acidic pH ranges where maximum phosphate sorption occurs (4–6, 10). Similar strategies for in situ immobilization of actinides by phosphate may be effective considering that actinide phosphates are highly insoluble and stable in geological formations (11).

Previous studies have shown uranyl to sorb moderately to  $\gamma$ -alumina, depending on pH, and generally find minimal sorption at acidic pH conditions (12–14). Phosphate and arsenate adsorb strongly to alumina at acidic to neutral pH values (15–17). In this study, we explored mechanisms for increasing U(VI) sorption under acidic pH conditions by pretreating  $\gamma$ -alumina surfaces with arsenate, a chemical analog of phosphate.  $\gamma$ -Alumina was chosen as the sorbent because of its high surface area and because its surface aluminol groups may be representative of those in aluminum-containing minerals, which are abundant in the environment and could serve in remediation strategies. Arsenate is not expected to be a viable candidate for pretreating soil and sediment minerals because of its potential release into the environment. However, as a chemical analog of phosphate, it offers the benefit of allowing more convenient characterization of the local structure of the reaction products by X-ray absorption spectroscopy (XAS) because of its stronger backscattering property and also higher absorption energy (K-edge, 11.876 keV) than that of phosphorus (K-edge, 2.149 keV). In the present study, we focus on the systematic examination of enhanced uranyl sorption by alumina surfaces pretreated with arsenate. A companion paper (14) provides detailed structural investigation of the sorption products, utilizing both U L<sub>III</sub>-edge and As K-edge EXAFS (extended X-ray absorption fine structure) spectroscopy, which allows direct characterization of uranyl–arsenate interactions at the alumina surface.

We also note a separate but parallel study, where we conducted experiments to examine the mechanism of arsenate and uranyl cosorption on  $\gamma$ -alumina surfaces at different solution conditions (18).

## 2. Materials and Methods

**2.1. Materials and Reagents.**  $\gamma$ - $Al_2O_3$  (aluminum oxide-C, purity >99.6%) was purchased from Degussa. The specific surface area measured by BET is  $100 \pm 15$  m<sup>2</sup>/g (provided by the manufacturer).  $\gamma$ -Alumina was aged at two concentration loadings (2 and 10 g/L) in a 0.01 M  $NaNO_3$  background electrolyte for ~1 month before sorption experiments were conducted. The pH of the initial suspensions was ~4.8–5.0. No further pH adjustments were made. After the aging process, measured pH was ~4.5–5.5. A portion of the aged suspension was centrifuged at 11000 rpm for 15 min, and then the wet paste was dried in air and ground for structural characterization. X-ray diffraction (XRD) analysis shows that the aged  $\gamma$ -alumina partially transformed to a mixture of bayerite and gibbsite polymorphs upon full hydration (Figure

\* Corresponding author phone: 617-496-3559; fax: 617-496-1023; e-mail: ytang@seas.harvard.edu.

<sup>†</sup> Current address: School of Engineering and Applied Science, Harvard University, 40 Oxford St., Cambridge, Massachusetts 02138.

SI-S1 of the Supporting Information), which is consistent with previous studies (16, 19–23).

American Chemical Society (ACS) grade sodium arsenate ( $\text{Na}_2\text{HAsO}_4 \cdot 6\text{H}_2\text{O}$ , Sigma) and uranyl nitrate ( $\text{UO}_2(\text{NO}_3)_2 \cdot 6\text{H}_2\text{O}$ , Alfa Aesar) were used for making arsenate (0.5 or 1 M, pH titrated to  $\sim 4$ ) and uranyl (0.1 or 0.5 M, no further pH adjustment) stock solutions. All experiments were conducted using boiled deionized (DI) water in a  $\text{N}_2$ -filled glovebox to minimize the effect of carbonate on arsenate sorption and its potential complexation with uranyl (24–26). The pH measurements were conducted using a Ag/AgCl glass electrode (Thermo Orion) and three-point calibration with buffered solutions pH 4, 7, and 10.

**2.2. Arsenate or Uranyl Sorption Experiments.** Three sets of sorption experiments were conducted for arsenate sorption on  $\gamma$ -alumina, including one sorption envelope experiment (alumina loading 10 g/L, As initial concentration 2 mM, and various pH values) and two sorption isotherm experiments at pH  $\sim 4$  (alumina loading 2 and 10 g/L, and As initial concentration 0.1–4 and 0.5–20 mM, respectively). Two sets of pH edge experiments were conducted for uranyl sorption on untreated  $\gamma$ -alumina (alumina loading 2 and 10 g/L, U initial concentration 0.2 and 1 mM, respectively).

For As or U sorption edge experiments, aged  $\gamma$ -alumina suspension was divided into several polypropylene high-speed centrifuge tubes (40 mL each). The pH of the suspension in each centrifuge tube was adjusted to the desired value (3.5–11.5), using 0.1 M  $\text{HNO}_3$  or NaOH. A predetermined volume of arsenate or uranyl stock solution was added to the suspension to achieve desired As or U concentrations. The suspension was then placed on a horizontal shaker and allowed to react for 24 h.

For As sorption isotherm experiments, 250 mL of aged  $\gamma$ -alumina suspension was titrated to pH  $\sim 4$  and divided into centrifuge tubes (40 mL each). Certain volumes of As stock solution were added in the suspension to achieve As initial concentrations of 0.1–20 mM. The pH was quickly adjusted using 0.1 M  $\text{HNO}_3$  or NaOH, if needed. The suspension was then allowed to react for 24 h while shaking.

After reaction, sorption products were centrifuged at 11000 rpm for 10 min. The supernatant was decanted and collected for As or U concentration analysis by direct current plasma atomic emission spectrometry (DCP-AES). The amount of As or U taken up by the alumina surface was expressed as percent uptake, calculated using the difference between As and U initial and final solution concentrations.

**2.3. Uranyl Sorption on Arsenate-Treated Alumina.** After the aging process, 250 mL  $\gamma$ -alumina suspension was titrated to pH  $4 \pm 0.2$  with 0.1 M NaOH or 0.1 M  $\text{HNO}_3$ , after which As stock solution was added to achieve As initial concentrations of 0.1–1 mM (the reason for choosing this concentration range will be discussed later). The pH was quickly adjusted if necessary. The suspension was allowed to react for 24 h while shaking. We refer to this procedure as the pretreatment (prt). After pretreatment, the pH of the suspension was measured, and 10 mL suspension was collected for As concentration analysis. The remainder of the suspension was divided into polypropylene centrifuge tubes (20 mL each), and a volume of U stock solution was added to each centrifuge tube to achieve U initial concentrations of 0.1–4 mM. The suspensions were then allowed to react for another 24 h and measured for final pH, followed by centrifugation, concentration, and structure analysis.

Parallel experiments with two alumina loadings (2 and 10 g/L) and corresponding ranges of  $[\text{As}]_{\text{ini}}$  and  $[\text{U}]_{\text{ini}}$  were carried out to examine the effects of relative As/U concentration ratios and absolute U concentrations. The choice of concentration ranges is discussed later. Sorption samples were labeled as prt–alumina loading (g/L)–As initial concentration (mM)–U initial concentration (mM). For example, prt–

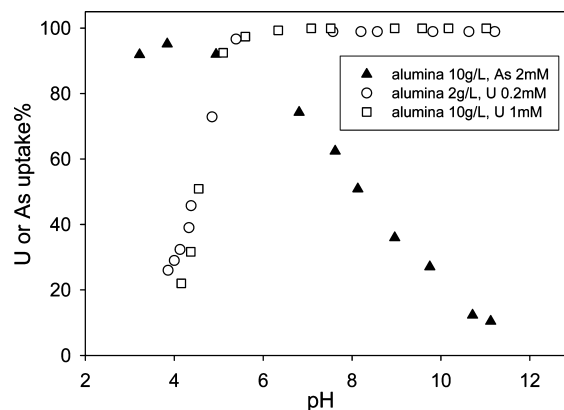


**FIGURE 1.** Arsenate and uranyl uptake (in separate experiments) on  $\gamma$ -alumina as a function of pH at different alumina loadings and As (or U) initial solution concentrations.

2–0.4–0.1 stands for a sorption sample with 2 g/L  $\gamma$ -alumina loading, 0.4 mM initial As concentration, and 0.1 mM initial U concentration.

**2.4. Kinetic Studies and Desorption Experiments.** Kinetic studies were performed on sample prt–2–0.4–0.1 to examine how readily U is taken up from the solution after the pretreatment by arsenate and addition of uranyl. Desorption experiments were carried out on sample series prt–2–0.4–0.1 and prt–2–0.4–0.4 to test long-term stability of the sorption products. Experimental details can be found in the Supporting Information.

### 3. Results and Discussion

**3.1. Arsenate or Uranyl Sorption on Alumina.** Sorption edges of uranyl and arsenate on  $\gamma$ -alumina from separate experiments are shown in Figure 1. Arsenate sorption reaches a maximum below pH 5, while uranyl sorption approaches a minimum ( $\sim 25\%$ ) at this pH range, consistent with previous studies (13, 16). Therefore, we selected pH 4, corresponding to maximal arsenate coverage, as the condition to evaluate whether pretreatment enhances uranyl uptake. We note that in addition to the formation of mononuclear and (or) binuclear inner sphere sorption complexes, when sorbed onto mineral surfaces, uranyl is known to form polymeric–colloidal phases or oxyhydroxide precipitates at neutral to basic pH ranges or at high U concentrations (12, 13, 27, 28). Therefore, the choice of pH 4 also minimizes the potential for formation of uranyl polymeric species due to pH effects. However, as we indicated previously, the use of parallel pretreatment sample series with different alumina loadings (2 and 10 g/L) and corresponding As and U initial concentration ranges allows us to examine the effect of absolute concentrations.

To evaluate the effect of surface-sorbed arsenate on uranyl uptake as well as the potential direct formation of uranyl arsenate precipitates directly from solution at high  $[\text{As}]_{\text{ini}}$ , it is important to estimate the density of surface adsorption sites on  $\gamma$ -alumina and the amount of arsenate needed for maximum surface coverage. Because of the complexity raised by surface transformation of  $\gamma$ -alumina into a gibbsite–bayerite mixture upon hydration (20–23), it was difficult to calculate the amount of arsenate needed for such requirements. Previous studies (29–31) reported values of 1.03–2 proton active sites per  $\text{nm}^2$  on  $\gamma$ -alumina as summarized in Table SI-S1 of the Supporting Information. On the basis of these numbers, the minimum amount of arsenate needed for maximum coverage (i.e., one As atom per site) is estimated to be 0.34–0.65 and 1.7–3.25 mM for 2 and 10 g/L alumina loading, respectively. We also took an experimental approach to address this question as discussed below.

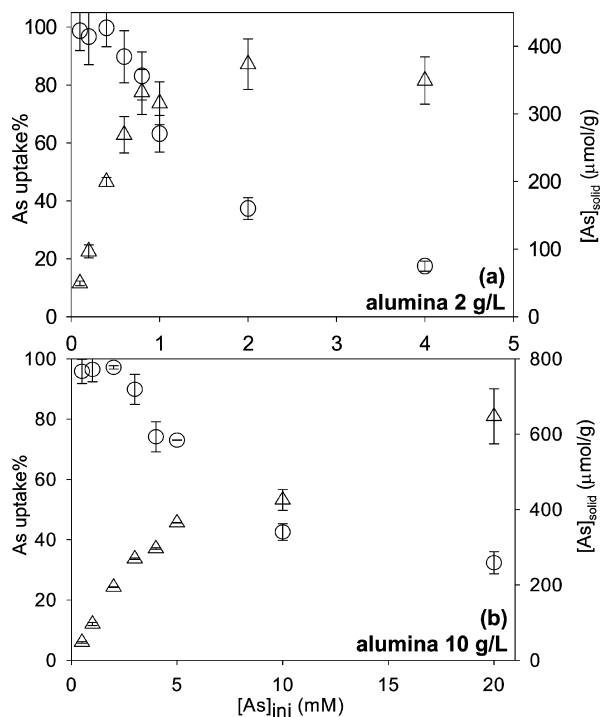


**FIGURE 2.** Arsenate percent uptake (○) and surface loading (△, expressed as  $[As]_{solid}$ ) as a function of initial As concentration,  $[As]_{ini}$ , for alumina loadings of (a) 2 g/L and (b) 10 g/L.

Sorption isotherms and percent uptake of As on the alumina surface at two alumina loadings (2 and 10 g/L) are shown in Figure 2. Both isotherms show a gradual increase of As uptake on alumina (expressed as  $[As]_{solid}$ , in  $\mu\text{mol/g}$ ), with increasing As initial concentration (expressed as  $[As]_{ini}$ , in mM). For 2 g/L alumina loading, a plateau at  $[As]_{ini} > 1.5$  mM follows the initial increase, suggesting saturation of available surface adsorption sites. For sample series with 10 g/L alumina loading, a sharp increase of  $[As]_{solid}$  is also observed at  $\sim 20$  mM after the plateau, suggesting the possible formation of surface precipitates.

On the basis of the surface site estimation and sorption isotherms, we chose the following  $[As]_{ini}$  ranges for pretreatment. For alumina loading of 2 g/L,  $[As]_{ini}$  is varied between 0.1 and 1 mM. As shown in Figure 2a, at  $[As]_{ini} < 0.4$  mM, more than 95% As is sorbed on the surface, leaving minimal As in the solution, thereby minimizing the potential for direct complexation and precipitation from the solution. Therefore, the concentration range of  $[As]_{ini} < 0.4$  mM allows examination of the effect of surface-sorbed As. For  $0.4 < [As]_{ini} < 1$  mM, a fraction of As is left in the solution. This allows the examination of combined effects of surface-sorbed and aqueous As. Similar strategies were used for alumina loading of 10 g/L (Figure 2b), with two concentration ranges of  $[As]_{ini} < 3$  mM (with more than 95% uptake) and  $3 < [As]_{ini} < 5$  mM (with a fraction of As remaining in solution).

**3.2. Aqueous Speciation.** Aqueous speciation of uranyl for the experimental conditions was calculated using the program PHREEQC (32) with the LLNL database provided with the program. Rutsch et al. (33) studied the formation constants of three uranyl arsenate aqueous complexes,  $\text{UO}_2\text{H}_2\text{AsO}_4^-$ ,  $\text{UO}_2\text{HAsO}_4^{0(aq)}$ , and  $\text{UO}_2(\text{H}_2\text{AsO}_4)_2^{0(aq)}$ , using time-resolved laser-induced fluorescence spectroscopy (TRLFS), and found their values to be similar to those of uranyl phosphate complexes  $\text{UO}_2\text{H}_2\text{PO}_4^-$ ,  $\text{UO}_2\text{HPO}_4^{0(aq)}$ , and  $\text{UO}_2(\text{H}_2\text{PO}_4)_2^{0(aq)}$ . Because limited solubility data were found for uranyl arsenate solid phases and because of the complexity introduced by the surface transformation of  $\gamma$ -alumina and pretreatment procedures (i.e., the presence of preadsorbed arsenate), we conducted speciation calculations for three

relevant systems, involving gibbsite, phosphate, and uranyl as likely guides for the  $\gamma$ -alumina–arsenate–uranyl system. They are (1) P(V) equilibrated with gibbsite, (2) U(VI) in the solution of interest, and (3) a system containing only aqueous uranyl and phosphate ions under the experimental conditions of pH 4 and  $\text{NaNO}_3$  0.01 M. Three representative P and U concentrations (0.1, 0.4, and 2 mM) were used for calculations. Aqueous speciation and saturation indexes with respect to solid phases are shown in Table 1.

In the gibbsite–P(V) system, at all P concentrations, the dominant aqueous species is  $\text{H}_2\text{PO}_4^-$ , with small amounts of  $\text{AlHPO}_4^-$ . Berlinite ( $\text{AlPO}_4$ ) becomes slightly oversaturated only at high P concentrations ( $> 2$  mM). In the U(VI) only system, the  $\text{UO}_2^{2+}$  species is dominant. At higher concentrations ( $> 2$  mM), polymeric species such as  $(\text{UO}_2)_2(\text{OH})_2^{2+}$  become important, resulting in potential precipitation of uranyl oxyhydroxide species such as schoepite and  $\text{UO}_3 \cdot 2\text{H}_2\text{O}$ . In the P(VI)–U(VI) system, depending on P and U concentrations, uranyl–phosphate complexes ( $\text{UO}_2\text{HPO}_4^{0(aq)}$  and  $\text{UO}_2\text{H}_2\text{PO}_4^-$ ) and  $\text{UO}_2^{2+}$  are the most dominant species, with  $(\text{UO}_2)_2(\text{OH})_2^{2+}$  increasing slightly at high U concentrations. These results indicate strong complexation between uranyl and phosphate ions in the solution, also suggesting the potential for formation of surface complexes or precipitates on the pretreated alumina surface. Saturation index calculations also indicate  $(\text{UO}_2)_3(\text{PO}_4)_2 \cdot 4\text{H}_2\text{O}$  as being the most oversaturated phase, followed by uranyl hydrogen phosphate compounds with different hydration states. As shown in the gibbsite–P(V) system,  $\text{AlPO}_4$  formation is possible at high P concentrations. Arai and Sparks (34) studied the effects of residence time on arsenate sorption on  $\gamma$ -alumina, using similar conditions as in our experiments (5 g/L alumina aged 1 month with 0.1 M NaCl, 1 mM initial As concentration, and pH 4.5). Their XANES results show the formation of only surface-sorbed species up to 3 days, and possible formation of mansfieldite-like precipitates ( $\text{AlAsO}_4 \cdot 2\text{H}_2\text{O}$ ) or rearrangements in the local structure of sorbed species for a longer reaction time (11 months). Laiti et al. (30, 35) studied the precipitation of aluminum phosphate phases during phosphate sorption on the alumina surface and suggested possible precipitation at high P/surface site ratios and long reaction times. Their adsorption data show no significant amount of P loss due to precipitation within 25 h. In light of these previous studies, for the conditions and pretreatment times (24 h) we employed, we do not expect any significant surface precipitation to have occurred. However, it is not possible to rule out minor precipitation. These speciation results for the phosphate system are intended as a first-approximation model for the corresponding arsenate system, which is the focus of this paper.

**3.3. Uranyl Sorption on Pretreated Alumina.** Kinetics of uranyl sorption on the pretreated alumina surface was studied for sample prt-2-0.4-0.1 (Figure SI-S2 of the Supporting Information). Percent uranyl uptake gradually increases within the initial 10 h and is followed by a plateau indicating a reaction steady state. Therefore, our choice of a 24 h reaction time should allow for an apparent steady state of uranyl sorption on the pretreated surfaces.

After careful examination of the sorption data over a range of  $\gamma$ -alumina loadings and As and U concentrations, some general trends are observed and are explained below.

**3.3.1. Effect of  $[As]_{ini}/[U]_{ini}$  Ratio.** Figure 3a shows that U percent uptake is positively related to the  $[As]_{ini}/[U]_{ini}$  ratio, with a gradual initial increase and a plateau at high  $[As]_{ini}/[U]_{ini}$  ratios. The  $[As]_{ini}/[U]_{ini}$  ratio is defined as the ratio between the initial As concentration for the pretreatment and the initial U solution concentration (both in mM). The U percent uptake on the untreated alumina surface is 20–25% at pH 4 (Figure 1 and dashed arrow C in Figure 3a). After pretreatment, for alumina loading of 2 g/L, the U percent



**TABLE 1. Speciation Calculations at Representative Experimental Conditions**

Gibbsite–P(V) system				U(VI) system					
[P] (mM)	0.1	0.4	2.0	[U] (mM)	0.1	0.4	2.0		
<b>P aqueous species (&gt;2%)</b>				<b>U aqueous species (&gt;2%)</b>					
H <sub>2</sub> PO <sub>4</sub> <sup>-</sup>	83.8	91.3	96.6	UO <sub>2</sub> <sup>2+</sup>	90.4	82.1	61.0		
AlHPO <sub>4</sub> <sup>+</sup>	15.5	8.1	2.8	UO <sub>2</sub> OH <sup>+</sup>	5.3	4.6	3.1		
				(UO <sub>2</sub> ) <sub>2</sub> (OH) <sub>2</sub> <sup>2+</sup>		5.5	13.5		
<b>S.I.<sup>a</sup> of solid phases</b>				<b>S.I.<sup>a</sup> of solid phases</b>					
AlPO <sub>4</sub> <sup>b</sup>			0.3	schoepite			0.1		
				UO <sub>3</sub> ·2H <sub>2</sub> O			0.1		
P(V)–U(VI) system									
[P] (mM)	0.1	0.1	0.1	0.4	0.4	0.4	2.0	2.0	2.0
[U] (mM)	0.1	0.4	2.0	0.1	0.4	2.0	0.1	0.4	2.0
<b>U aqueous species (&gt;2%)</b>									
UO <sub>2</sub> HPO <sub>4</sub> <sup>0(aq)</sup>	66.3	20.7	4.2	80.9	74.5	16.8	71.5	73.4	78.9
UO <sub>2</sub> H <sub>2</sub> PO <sub>4</sub> <sup>+</sup>	11.5	3.6		14.0	12.9	3.0	12.6	13.0	13.8
UO <sub>2</sub> <sup>2+</sup>	20.3	63.9	58.7		11.0	51.7			5.4
UO <sub>2</sub> (H <sub>2</sub> PO <sub>4</sub> ) <sub>2</sub> <sup>0(aq)</sup>				2.8			15.2	12.9	
UO <sub>2</sub> OH <sup>+</sup>		3.6	3.0			2.7			
(UO <sub>2</sub> ) <sub>2</sub> (OH) <sub>2</sub> <sup>2+</sup>		3.4	12.6			10.0			
<b>S.I.<sup>a</sup> of solid phases</b>									
(UO <sub>2</sub> ) <sub>3</sub> (PO <sub>4</sub> ) <sub>2</sub> ·4H <sub>2</sub> O	5.1	6.4	7.0	4.2	6.7	8.1	3.3	5.2	8.6
H <sub>2</sub> (UO <sub>2</sub> ) <sub>2</sub> (PO <sub>4</sub> ) <sub>2</sub> <sup>c</sup>	0.1	0.3	0.3	0.3	1.4	1.5	0.2	1.4	2.9
UO <sub>2</sub> HPO <sub>4</sub>	0.1	0.2	0.2	0.2	0.7	0.8	0.1	0.7	1.4
UO <sub>2</sub> HPO <sub>4</sub> ·4H <sub>2</sub> O <sup>d</sup>	0.4	0.5	0.5	0.5	1.1	1.1	0.4	1.1	1.8

<sup>a</sup> Saturation index (S.I.) = log(Q/K<sub>eq</sub>). <sup>b</sup> Mineral berlinite. <sup>c</sup> Mineral autunite. <sup>d</sup> Mineral chernikovite.

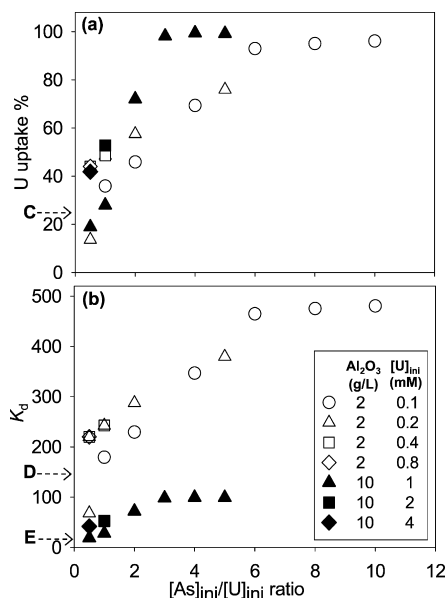


**FIGURE 3. (a) U percent uptake and (b) partition coefficient,  $K_d$ , as a function of the  $[As]_{ini}/[U]_{ini}$  ratio for two alumina loadings (2 and 10 g/L) and  $[U]_{ini} = 0.1$ –4 mM.  $[As]_{ini}/[U]_{ini}$  is defined as the ratio between the initial As pretreatment concentration and the initial U concentration (both in mM).  $K_d$  is defined as the ratio between  $[U]_{solid}$  ( $\mu\text{mol/g}$ ) and  $[U]_{ini}$  (mM). Dashed arrow C indicates the percent uptake value of U on an untreated alumina surface (Figure 1). Horizontal dashed arrows D and E indicate  $K_d$  values of U sorption on untreated alumina for 2 g/L loading and U 0.2 mM and 10 g/L loading and U 1 mM, respectively.**

uptake is greatly increased to ~50% at a  $[As]_{ini}/[U]_{ini}$  ratio of 3 and reaches a plateau of ~90% at a  $[As]_{ini}/[U]_{ini}$  ratio > 7. For alumina loading of 10 g/L, a steeper trend is observed, with the percent U uptake of 50% at a  $[As]_{ini}/[U]_{ini}$  ratio of ~2, and U is almost depleted from the solution when the  $[As]_{ini}/[U]_{ini}$  ratio > 3.

**3.3.2. Effect of Absolute  $[As]_{ini}$  at Fixed  $[U]_{ini}$ .** A closer examination of the effect of absolute  $[As]_{ini}$  involves the two regions discussed in Section 3.1: (1) a low  $[As]_{ini}$  region, where almost all As is sorbed on the surface, and (2) a higher  $[As]_{ini}$  region, where high surface coverage of As is obtained but considerable As remains in solution. Absolute  $[As]_{ini}$  can be readily calculated on the basis of the  $[As]_{ini}/[U]_{ini}$  ratio and  $[U]_{ini}$ , shown in the legend of Figure 3a. For alumina loading of 2 g/L, the low  $[As]_{ini}$  region is considered as  $[As]_{ini} < 0.4$  mM, where more than 95% is sorbed during the pretreatment process (Figure 2). Figure 3a shows that in this region, U percent uptake is enhanced at different degrees depending on  $[U]_{ini}$ . For example, for 0.1 mM  $[U]_{ini}$ , U percent uptake is enhanced to ~70% at 0.4 mM  $[As]_{ini}$  ( $[As]_{ini}/[U]_{ini} = 4$ ), whereas for 0.2 mM  $[U]_{ini}$ , U percent uptake is ~60% at  $[As]_{ini} = 0.4$  mM ( $[As]_{ini}/[U]_{ini} = 2$ ). This suggests that the pretreated alumina surface has a much stronger affinity for uranyl sorption either because of its electrostatic attraction to the surface-sorbed negatively charged arsenate or because of the formation of ternary surface complexes and/or precipitates. In the higher  $[As]_{ini}$  region of 0.4–1 mM, a fraction of As remains in the solution, and U uptake increases until reaching a plateau, where it is almost completely removed from the solution. In this region, despite the effects of the surface-sorbed arsenate mentioned above, complexation and/or precipitation of uranyl arsenate species from the solution are also likely to be important. Similar trends are also observed for sample series with alumina loading of 10 g/L in regions where  $[As]_{ini} < 3$  mM and  $3 < [As]_{ini} < 5$  mM.

**3.3.3. Effect of Alumina Loading.** At a given  $[As]_{ini}/[U]_{ini}$  ratio, higher alumina loading (10 g/L) yields a higher U percent uptake (Figure 3a) until 100% U uptake is reached. This is likely due to the increased surface area with increased alumina loading. In order to eliminate the effect of alumina loading, we used a partition coefficient,  $K_d$ , defined as

$$K_d = \frac{[U]_{solid}(\mu\text{mol g}^{-1})}{[U]_{ini}(\text{mmol L}^{-1})} \quad (1)$$

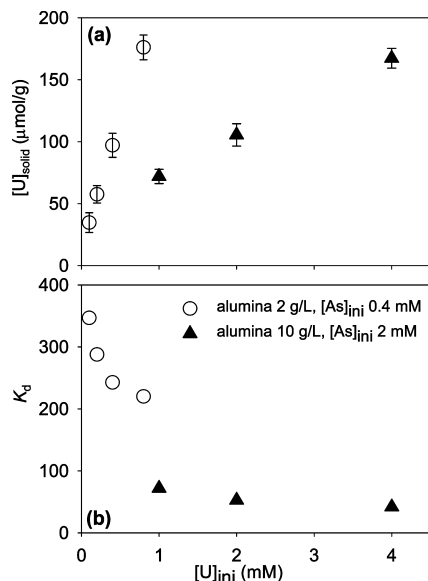


**FIGURE 4.** (a) U surface loading on pretreated alumina, expressed as  $[U]_{\text{solid}}$  ( $\mu\text{mol/g}$ ) and (b) U partition coefficient  $K_d$  on the arsenate-pretreated alumina surface as a function of initial U concentration. Open  $\circ$  show alumina loading of 2 g/L and  $[\text{As}]_{\text{ini}}$  0.4 mM, i.e., sample series prt-2-0.4- $[U]_{\text{ini}}$ . Solid  $\blacktriangle$  show alumina loading of 10 g/L and  $[\text{As}]_{\text{ini}}$  2 mM, i.e., sample series prt-10-2- $[U]_{\text{ini}}$ .

which normalizes U uptake to alumina loading and expresses the partitioning of U between solid and solution. The plot of  $K_d$  as a function of  $[\text{As}]_{\text{ini}}/[U]_{\text{ini}}$  is shown in Figure 3b. For certain alumina loading, similar trends are shown as observed for the U percent uptake, where an increase in the  $[\text{As}]_{\text{ini}}/[U]_{\text{ini}}$  ratio results in an increased  $K_d$  value as compared to the  $K_d$  values of U sorption on untreated alumina surfaces at 2 and 10 g/L (values indicated by dashed arrows D and E in Figure 3b, respectively). However, comparing  $K_d$  values for sample series with different alumina loadings shows that the sample series with low alumina loading (2 g/L) exhibits much higher U partitioning (almost 5-fold more) between the solid and liquid phase as compared to that of the sample series with high alumina loading (10 g/L). This is likely due to the high U concentrations used at high alumina loading.

**3.3.4. Effect of  $[U]_{\text{ini}}$  at Fixed  $[\text{As}]_{\text{ini}}$ .** Figure 4a shows U surface loading on arsenate-treated alumina as a function of  $[U]_{\text{ini}}$ . Sample series shown are alumina loading of 2 g/L with  $[\text{As}]_{\text{ini}} = 0.4$  mM (98.7% sorbed on surface) and alumina loading of 10 g/L with  $[\text{As}]_{\text{ini}} = 2$  mM (96.9% sorbed on surface). Increasing  $[U]_{\text{ini}}$  results in greater overall U uptake on the pretreated surface but decreased partitioning as seen by lower  $K_d$  values (Figure 4b). However, similar to the trend shown in Figure 3b, low alumina loading (2 g/L) generally results in greater partitioning of U between solid and liquid phases (higher  $K_d$  values) as compared to high alumina loading of 10 g/L.

**3.4. Desorption Experiments.** Results from desorption (prt) experiments conducted on two sample series (prt-2-0.4-0.1 and prt-2-0.4-0.4) are shown in Figure 5. The percentage of U remaining sorbed on the surface is normalized to the total amount of U taken up by alumina before desorption was initiated ( $\sim 70\%$  for prt-2-0.4-0.1 and  $\sim 49\%$  for prt-2-0.4-0.4 as shown in Figure 4a). In both samples,  $\sim 95\%$  of the As remains sorbed (as normalized to the initial amount taken up) throughout the whole desorption process, consistent with its strong affinity for the alumina surface at an acidic pH. For both series, the amount of sorbed U varies during the initial  $\sim 20$  h and only reaches apparent steady state slowly. After 192 h,  $\sim 50\%$  of the U is sorbed for

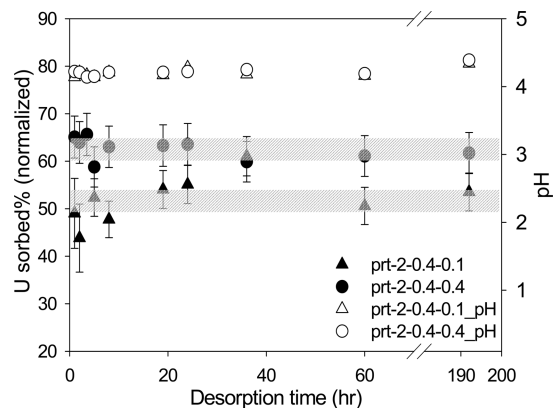


**FIGURE 5.** Percentage of uranyl that remains sorbed during desorption (normalized to the amount of U sorbed on a  $\gamma$ -alumina surface before desorption) and pH of the suspension as a function of desorption time for sample series prt-2-0.4-0.1 and prt-2-0.4-0.4.

prt-2-0.4-0.1 and  $\sim 65\%$  for dsp-2-0.4-0.4. Although desorption is known to be dependent upon experimental conditions and kinetics, these results nevertheless suggest that only a limited amount of the uranyl that has been sorbed on the surface is remobilized through the desorption process under these experimental conditions. This could be due to the formation of strong surface complexes such as an uranyl-arsenate ternary surface complex or the formation of uranyl arsenate surface precipitates as suggested by the speciation calculations. Investigation into the mechanisms of enhanced uranyl sorption as well as stability of sorption products is presented in a companion paper (14), in which X-ray absorption spectroscopy and X-ray diffraction were utilized for direct characterization of sorption products. These are found to be a mixture of surface adsorbed uranyl species and uranyl arsenate precipitates.

**3.5. Environmental Implications.** In this study, we demonstrated how pretreatment of alumina surface with a ligand having strong affinities for both the surface and uranyl can enhance uranyl uptake from solution and lead to more stable final sorption products. Arsenate was chosen as an analog for environmentally abundant and commercially accessible phosphate. Inasmuch as uranyl sorption on untreated alumina is not favored at low pH, the pretreatment procedure could significantly increase the efficiency of sorption on alumina. It is also likely to increase the stability of the sorption products, thereby limiting the remobilization of surface adsorbed uranium. The most important contribution of this work is the conceptual basis we provide for modifying surface properties of aluminum-rich solids to enhance their sorption selectivity and capacity over specific pH ranges. Although  $\gamma$ -alumina is an unlikely sorbent for remediation and was chosen as a model solid, we demonstrate that nearly a 5-fold enhancement in uranyl uptake can be achieved. Therefore, knowledge gained from this work may also have application for the design of materials for uranium remediation, especially under acidic conditions. Results from this work also provide predictive information of U(VI) mobility in complex natural systems, where ligands such as phosphate sorb onto mineral surfaces prior to exposure to U(VI).

To better understand the operative uptake mechanisms on a molecular scale, we investigated samples from the present paper using X-ray absorption spectroscopy and X-ray diffraction to assess local structure and long-range order of the sorption products. The results are presented in a companion paper (14).

## Acknowledgments

This work was supported by the Center for Environmental Molecular Science at SUNY-Stony Brook through National Science Foundation Grant CHE-0221924. We thank S. Cochiara and J. Feng (Department of Geosciences, SUNY-Stony Brook) for gibbsite and bayerite samples. Comments from two anonymous reviewers greatly improved the manuscript. We appreciate the efforts of Editor Dr. Ruben Kretzschmar in handling this manuscript.

## Supporting Information Available

Experimental details of kinetic studies and desorption experiments, table of  $\gamma$ -alumina surface site density, a figure of XRD patterns of aged  $\gamma$ -alumina, and a figure of U loading and partition coefficient on arsenate-pretreated alumina as a function of U initial concentration. This information is available free of charge via the Internet at <http://pubs.acs.org>.

## Literature Cited

- Duff, M. C.; Amrhein, C. Method for the separation of uranium (VI) and (VI) oxidation states in natural waters. *J. Chromatogr., A* **1996**, *743*, 335–340.
- Langmuir, D. *Aqueous Environmental Geochemistry*; Prentice-Hall, Inc.: Upper Saddle River, NJ, 1997; pp 495–512.
- Duff, M. C.; Coughlin, J. U.; Hunter, D. B. Uranium coprecipitation with iron oxide minerals. *Geochim. Cosmochim. Acta* **2002**, *66*, 3533–3547.
- Weesner, F. J.; Bleam, W. F. Binding characteristics of Pb<sup>2+</sup> on anion-modified and pristine hydrous oxide surfaces studied by electrophoretic mobility and X-ray absorption spectroscopy. *J. Colloid Interface Sci.* **1998**, *205*, 380–389.
- Wang, K.; Xing, B. Adsorption and desorption of cadmium by goethite pretreated with phosphate. *Chemosphere* **2002**, *48*, 665–670.
- Li, W.; Zhang, S.; Shan, X. Surface modification of goethite by phosphate for enhancement of Cu and Cd adsorption. *Colloids Surf., A* **2007**, *293*, 13–19.
- Yoon, S. J.; Helmke, P. A.; Amonette, J. E.; Bleam, W. F. X-ray absorption and magnetic studies of trivalent lanthanide ions sorbed on pristine and phosphate-modified boehmite surfaces. *Langmuir* **2002**, *18*, 10128–10136.
- Adebowale, K. O.; Unuabonah, I. E.; Olu-Owolabi, B. I. Adsorption of some heavy metal ions on sulfate- and phosphate-modified kaolin. *Appl. Clay Sci.* **2005**, *29*, 145–148.
- Unuabonah, E. I.; Adebowale, K. O.; Olu-Owolabi, B. I. Kinetic and thermodynamic studies of the adsorption of lead (II) ions onto phosphate-modified kaolinite clay. *J. Hazard. Mater.* **2007**, *144*, 386–395.
- Ranatunga, T. D.; Taylor, R. W.; Schulthess, C. P.; Ranatunga, D. R. A.; Bleam, W. F.; Senwo, Z. N. Lead sorption on phosphate-pretreated kaolinite: Modeling, aqueous speciation, and thermodynamics. *Soil Sci.* **2008**, *173*, 321–331.
- Liu, X. W.; Byrne, R. H. Rare earth and yttrium phosphate solubilities in aqueous solution. *Geochim. Cosmochim. Acta* **1997**, *61*, 1625–1633.
- Sylwester, E. R.; Hudson, E. A.; Allen, P. G. The structure of uranium(VI) sorption complexes on silica, alumina, and montmorillonite. *Geochim. Cosmochim. Acta* **2000**, *64*, 2431–2438.
- Froideval, A.; Nero, M. D.; Gaillard, C.; Barillon, R.; Rossini, I.; Hazemann, J. L. Uranyl sorption species at low coverage on Al-hydroxide: TRLFS and XAFS studies. *Geochim. Cosmochim. Acta* **2006**, *70*, 5270–5284.
- Tang, Y.; MacDonald, J.; Reeder, R. J. Enhanced uranium sorption on aluminum oxide pretreated with arsenate. Part II: Spectroscopic studies. *Environ. Sci. Technol.* 2009, DOI: 10.1021/es802370d.
- Guo, Z. J.; Yu, X. M.; Guo, F. H.; Tao, Z. Y. Th(IV) adsorption on alumina: Effects of contact time, pH, ionic strength, and phosphate. *J. Colloid Interface Sci.* **2005**, *288*, 14–20.
- Arai, Y.; Elzinga, E. J.; Sparks, D. L. X-ray absorption spectroscopic investigation of arsenate and arsenite adsorption at the aluminum oxide–water interface. *J. Colloid Interface Sci.* **2001**, *235*, 80–88.
- Goldberg, S.; Johnston, C. T. Mechanisms of arsenic adsorption on amorphous oxides evaluated using macroscopic measurements, vibrational spectroscopy, and surface complexation modeling. *J. Colloid Interface Sci.* **2001**, *234*, 204–216.
- Tang, Y.; Reeder, R. J. Uranyl and arsenate sorption on aluminum oxide. *Geochim. Cosmochim. Acta* **2009**, *73*, 2727–2743.
- Wijnja, H.; Schulthess, C. P. ATR-FTIR and DRIFT spectroscopy of carbonate species at the aged  $\gamma$ -Al<sub>2</sub>O<sub>3</sub>–water interface. *Spectrochim. Acta A* **1999**, *55*, 861–872.
- Paglia, G.; Bozin, E. S.; Billinge, S. J. L. Fine-scale nanostructure in  $\gamma$ -Al<sub>2</sub>O<sub>3</sub>. *Chem. Mater.* **2006**, *18*, 3242–3248.
- Roelofs, F.; Vogelsberger, W. Dissolution kinetics of nanodispersed  $\gamma$ -alumina in aqueous solution at different pH: Unusual kinetic size effect and formation of a new phase. *J. Colloid Interface Sci.* **2006**, *303*, 450–459.
- Yang, X.; Sun, Z.; Wang, D.; Forsling, W. Surface acid–base properties and hydration–dehydration mechanisms of aluminum (hydr)oxides. *J. Colloid Interface Sci.* **2007**, *308*, 395–404.
- Carrier, X.; Marceau, E.; Lambert, J. F.; Che, M. Transformations of  $\gamma$ -alumina in aqueous suspensions I. Alumina chemical weathering studied as a function of pH. *J. Colloid Interface Sci.* **2007**, *308*, 429–437.
- Bargar, J. R.; Reitmeyer, R.; Davis, J. A. Spectroscopic confirmation of uranium(VI)–carbonate adsorption complexes on hematite. *Environ. Sci. Technol.* **1999**, *33*, 2481–2484.
- Bargar, J. R.; Reitmeyer, R.; Lenhart, J. J.; Davis, J. A. Characterization of U(VI)–carbonate ternary complexes on hematite: EXAFS and electrophoretic mobility measurements. *Geochim. Cosmochim. Acta* **2000**, *64*, 2737–2749.
- Elzinga, E. J.; Tait, C. D.; Reeder, R. J.; Rector, K. D.; Donohoe, R. J.; Morris, D. E. Spectroscopic investigation of U(VI) sorption at the calcite–water interface. *Geochim. Cosmochim. Acta* **2004**, *68*, 2437–2448.
- Kowal-Fouchard, A.; Drot, R.; Simoni, E.; Ehrhardt, J. J. Use of spectroscopic techniques for uranium(VI)/montmorillonite interaction modeling. *Environ. Sci. Technol.* **2004**, *38*, 1399–1407.
- Baumann, N.; Brendler, V.; Arnold, V.; Geipel, G.; Bernhard, G. Uranyl sorption onto gibbsite studied by time-resolved laser-induced fluorescence spectroscopy (TRLFS). *J. Colloid Interface Sci.* **2005**, *290*, 318–324.
- Kummert, R.; Stumm, W. The surface complexation of organic acids on hydrous  $\gamma$ -Al<sub>2</sub>O<sub>3</sub>. *J. Colloid Interface Sci.* **1980**, *75*, 373–385.
- Laiti, E.; Persson, P.; Ohman, L. O. Surface complexation and precipitation at the H<sup>+</sup>-orthophosphate-aged  $\gamma$ -Al<sub>2</sub>O<sub>3</sub>–water interface. *Langmuir* **1996**, *12*, 2969–2975.
- Lefevre, G.; Duc, M.; Lepeut, P.; Caplain, R.; Fedoroff, M. Hydration of  $\gamma$ -alumina in water and its effects on surface reactivity. *Langmuir* **2002**, *18*, 7530–7537.
- Parkhurst, D. L.; Appelo, C. A. J. *User's Guide to PHREEQC: A Computer Program for Speciation, Batch Reaction, One-Dimensional Transport, and Inverse Geochemical Calculations*, version 2; U. S. Geological Survey, Water Resources Investigations Report 99-4259; Denver, CO, 1999; p 310.
- Rutsch, M.; Geipel, G.; Brendler, V.; Bernhard, G.; Nitsche, H. Interaction of uranium(VI) with arsenate(V) in aqueous solution studied by time-resolved laser-induced fluorescence spectroscopy (TRLFS). *Radiochim. Acta* **1999**, *86*, 135–141.
- Arai, Y.; Sparks, D. L. Residence time effects on arsenate surface speciation at the aluminum oxide–water interface. *Soil Sci.* **2002**, *167*, 303–314.
- Laiti, E.; Persson, P.; Ohman, L. O. Balance between surface complexation and surface phase transformation at the alumina–water interface. *Langmuir* **1998**, *14*, 825–831.

ES802369M